

Numerical Investigation of Surface Plasmons Associated Subwavelength Optical Single-Pass Effect *

MIN Chang-Jun(闵长俊), WANG Pei(王沛), JIAO Xiao-Jin(焦小瑾), MING Hai(明海)**

Institute of Photonics, University of Science and Technology of China, Hefei 230026

(Received 13 June 2007)

Surface plasmons (SPs) associated optical single-pass effect has been investigated in novel subwavelength metallic structures, including single slit and grating structures. With influence of SPs, these metallic structures can enhance transmission in incident direction and suppress it in the opposite direction, exhibiting a single-pass effect. The finite difference time domain method is employed to study the influences of structure parameters on far-field transmission, near-field electric field distribution and extinction ratio of the single-pass transmission effect. A maximal extinction ratio of 47.83 dB is achieved in the grating structure.

PACS: 71.36.+c, 73.20.Mf, 78.66.Bz, 42.25.Fx

Since Ebbesen *et al.*^[1] first reported the extraordinary optical transmission through a two-dimensional hole array perforated on a metallic film, there has been an explosion of interest in the interaction between light and subwavelength metallic structures.^[2,3] Arrays of nanoholes or slits perforated in metallic films, as well as single nano-apertures or dressed by shallow corrugation, are currently investigated from visible to microwave frequencies.^[4-7] The excitation of surface plasmons (SPs) has been promoted as the primary vector responsible for the interaction between light and nano-objects.^[2-11] The enhancement of SPs to optical transmission has attracted considerable interest and produced many related applications.^[7-9] However, recent experimental and theoretical studies^[10,11] have revealed that SPs can also suppress the transmission in some simple structures, such as groove-slit and hole-slit structures, which may contribute to new applications.

In this Letter, we try to realize the fundamentals of the interaction between light and nano-objects, study new phenomena and develop new applications. Several novel subwavelength metallic structures are specifically investigated, including single slit and grating structures, in which SPs can be excited in suitable wavelengths. With influence of SPs, the transmission in these structures can be enhanced in incident direction and suppressed in opposite direction, exhibiting a single-pass transmission phenomenon. The phenomenon has great potential applications for designing nano-optical devices in signal transmission and isolation, etc.

Two-dimensional finite difference time domain (FDTD) method^[13] is used in our work with the cell $5 \text{ nm} \times 5 \text{ nm}$. The second-order Lorentz dispersion model^[14] is used to simulate the metallic film. The

periodic boundary conditions (PBC)^[15] and perfectly matched layer (PML)^[16] are used in boundaries of the simulated area. In our simulation, the normal incident TM-polarized plane wave illuminates the metallic structures vertically with wavelength $\lambda = 850 \text{ nm}$. The metal used here is Ag and the permittivity takes the values from Ref. [12].

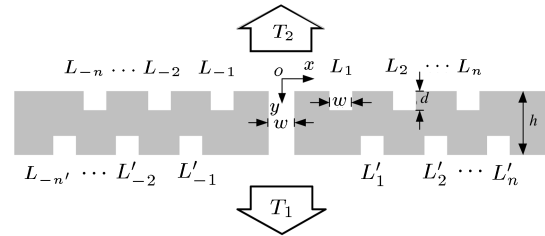


Fig. 1. Schematically single slit structure with grooves on both upper and under surfaces. The parameters are taken as the thickness of Ag film $h = 200 \text{ nm}$, the width of both slit and groove $w = 100 \text{ nm}$ and the groove depth $d = 100 \text{ nm}$. The TM-polarized plane wave illuminates the structure vertically with wavelength $\lambda = 850 \text{ nm}$.

We investigate the SPs associated optical single-pass effect in a single slit structure. The schematically single slit structure is shown in Fig. 1, which is comprised of a subwavelength slit in the Ag film and some grooves on both the upper and lower surfaces. The grooves on upper surface are used to excite SPs and to enhance the transmission from top to bottom (denoted as T_1 in Fig. 1). The positions of grooves in the x direction on the upper surface (denoted as $L_{-n}, \dots, L_{-2}, L_{-1}, L_1, L_2, \dots, L_n$ in Fig. 1) are chosen as $L_n = L_1 + (n - 1)\lambda_{sp}$ and $L_{-n} = -L_n$. Subscript n denotes the number of grooves on one side of slit. $L_1 = 500 \text{ nm}$ is the position of the first groove obtained from the first transmission peak of the groove-slit structure in Ref. [11]. Here

* Supported by the National Natural Science Foundation of China under Grant No 10474093, and the National Basic Research Programme of China under Grant No 2006CB302905.

** Email: minghai@ustc.edu.cn

©2007 Chinese Physical Society and IOP Publishing Ltd

$\lambda_{sp} = 840$ nm is the wavelength of SPs on a plane silver surface with incident light $\lambda = 850$ nm. According to Ref. [11], the grooves on the upper surface all distribute in the just positions to enhance the transmission T_1 through the slit. Contrarily, the grooves on the lower surface all distribute in the positions to suppress the transmission through slit in reverse direction (denoted as T_2 in Fig. 1). The respective positions of grooves on the lower surface (denoted as

$L'_{-n}, \dots, L'_{-2}, L'_{-1}, L'_1, L'_2, \dots, L'_n$ in Fig. 1) are chosen as $L'_n = L'_1 + (n-1)\lambda_{sp}$ and $L'_{-n} = -L'_n$. The position of the first groove, $L'_1 = 900$ nm, is obtained from the first minimal transmission of the groove-slit structure in Ref. [11]. Therefore light is allowed to transmit from top to bottom but prohibited in the reverse direction, which exhibits a single-pass effect. The extinction ratio is used here to scale the single-pass effect, which is defined as $10[\log(T_1/T_2)]$ in units of dB.

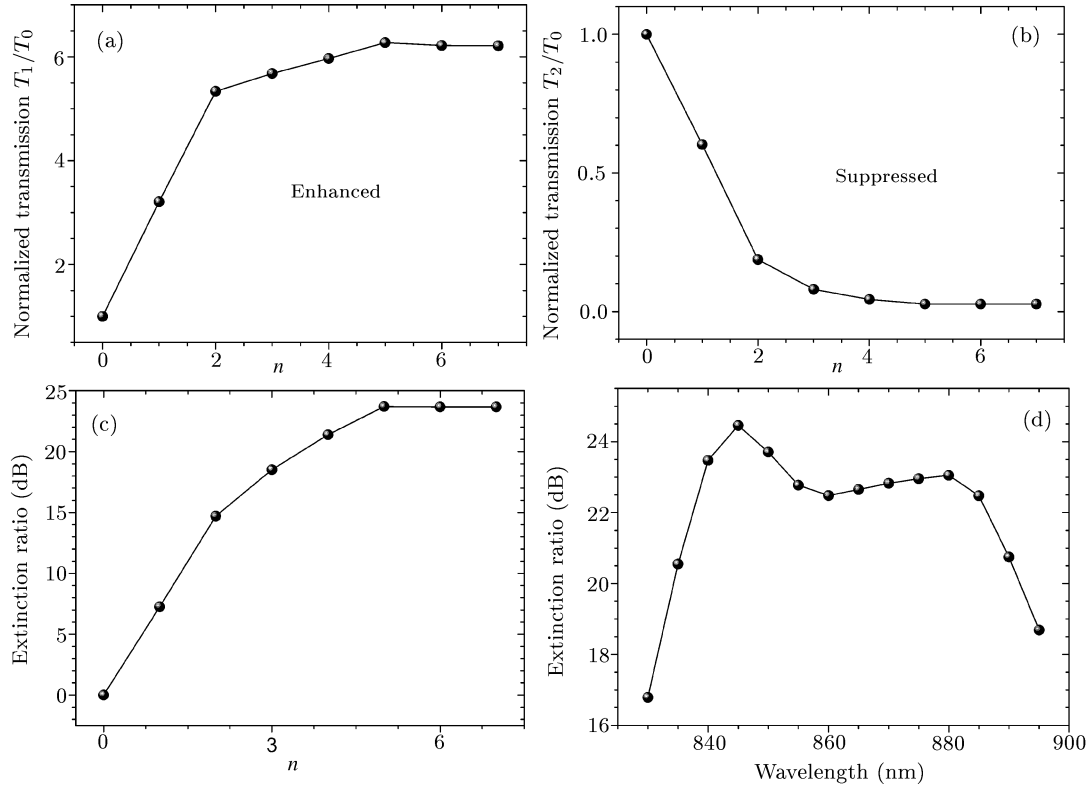


Fig. 2. Normalized transmission (a) T_1/T_0 and (b) T_2/T_0 versus the number n of grooves in the single slit structure. (c) Extinction ratio versus the number n of grooves in the single slit structure. (d) Extinction ratio versus the wavelength of incident light for $n = 5$.

Then we consider the influence of the grooves on far-field transmission in single slit structure. We first focus on the influence of the number n of grooves. Fig. 2(a) shows the normalized transmission T_1/T_0 as a function of the number of grooves n . T_0 denotes the transmission through a common single slit without grooves. It can be observed that the transmission is enhanced greatly by SPs as n increases, and the enhancement saturates at about $n = 5$, when T_1 is enhanced by a factor of 6.27. This is similar to the experimental result reported in Ref. [5]. The situation of normalized transmission T_2/T_0 is shown in Fig. 2(b), which presents the strong suppressed transmission caused by SPs as n increases. The suppression also saturates at about $n = 5$, when T_2 is suppressed by a factor of 0.0267. As a result of the effective enhancement and suppression of SPs to transmission, the extinction ratios of the isolator are obtained

as shown in Fig. 2(c). The maximal extinction ratio reaches 23.71 dB at $n = 5$. Figure 2(d) shows the extinction ratio at $n = 5$ as a function of the wavelength of incident light. In Fig. 2(d), the range of wavelength is more than 50 nm with the extinction ratio beyond 20 dB, which is quite wide.

The single slit structure can be applied in some subwavelength optical instruments. However, even enhanced by SPs, the transmission power through the single slit is not strong enough. In order to obtain both high extinction ratio and strong transmission power together, we consider the periodic slit structure (grating structure) in the following text.

Figure 3 shows the grating configuration designed, which is comprised of a silver grating with grooves. There are two grooves on upper surface and one groove on under surface between two slits. The same as the single slit structure, the grooves on upper surface can

enhance the transmission through slits from top to bottom (denoted as T_1), and the groove on under surface is used to suppress the transmission in opposite direction (denoted as T_2). The groove on under surface locates at the centre between two slits, hence the period of grating $p = 2L_2$.

The values $L_1 = 500$ nm and $L_2 = 900$ nm are chosen from the single slit structure above. However, they are not the best values in the grating structure, because the interaction between slits also plays an important role here. Thus the values of L_1 and L_2 are changed to study their effect to far-field transmission. Figure 4(a) shows the transmission T_2 as a function of L_2 . It can be observed that the transmission is remarkably suppressed at about $L_2 = 835$ nm with the minimum $T_2 = 4.52 \times 10^{-5}$. When $L_2 = 835$ nm, the grating period $p = 2L_2 \approx 2\lambda_{sp}$, which is similar to the result of two-slit structure as slit separation equal to $4\lambda_{sp}/2$ in Ref. [10]. They all present the suppressed effect by interaction of SPs between slits. Then we choose the grating period $p = 2L_2 = 1670$ nm constant, and change the slit-groove distance L_1 to study the enhancement of T_1 . Figure 4(b) shows the

transmission T_1 as a function of L_1 . The maximum $T_1 = 0.49$ is obtained at $L_1 = 570$ nm. Hence at the peak of Fig. 4(b), nearly 50% energy can be transmitted through the grating structure, which is rather stronger than the single slit structure.

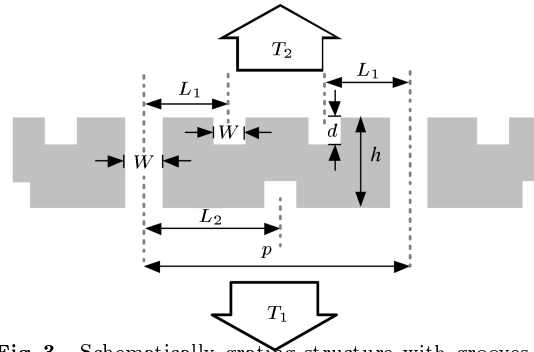


Fig. 3. Schematically grating structure with grooves on both upper and under surfaces. The lateral scale is two periods of grating. The parameters are chosen as the thickness of the grating $h = 200$ nm, the width of both slit and groove $w = 100$ nm, the groove depth $d = 100$ nm, the slit-groove distance $L_1 = 500$ nm on upper surface and $L_2 = 900$ nm on lower surface.

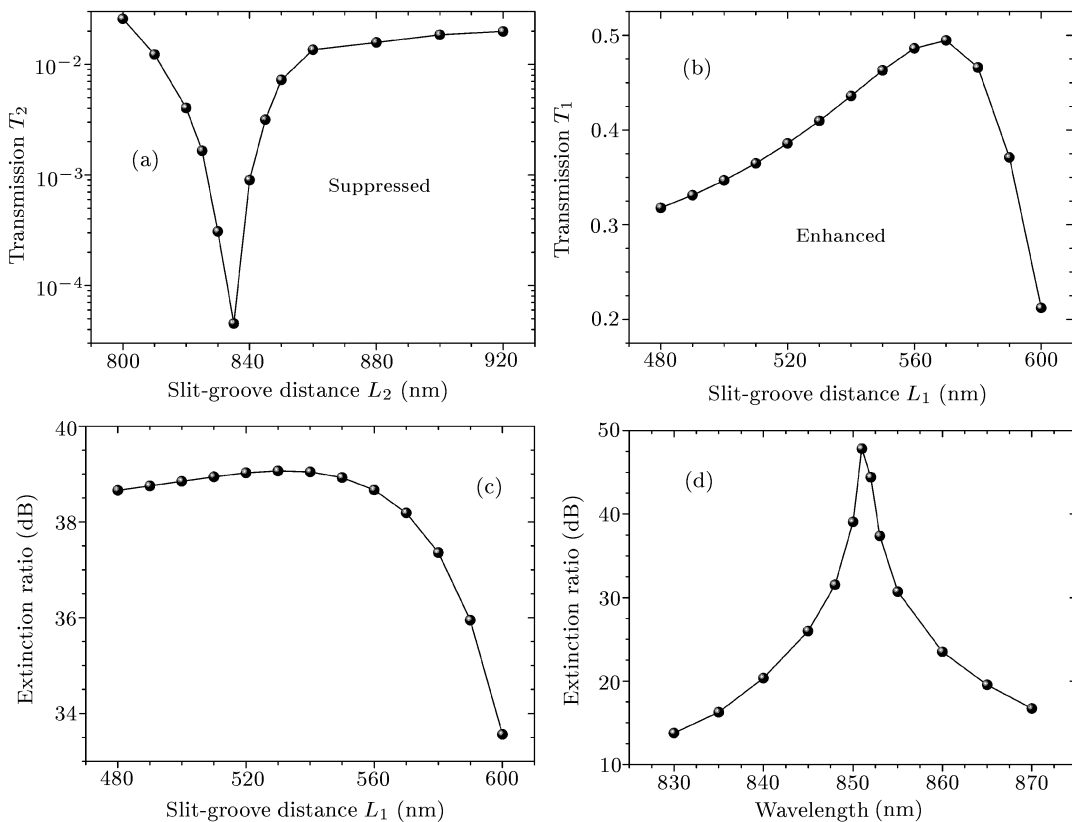


Fig. 4. (a) Transmission T_2 versus slit-groove distance L_2 on the lower surface. (b) Transmission T_1 versus slit-groove distance L_1 on the upper surface with $L_2 = 835$ nm. (c) Extinction ratio of grating structure as a function of L_1 with $L_2 = 835$ nm. (d) Extinction ratio as a function of the wavelength of incident light with $L_1 = 530$ nm and $L_2 = 835$ nm.

On account of more effective enhancement and suppression caused by SPs, the extinction ratio of grating structure is greater than the single slit structure. Figure 4(c) shows the extinction ratio as function of L_1 under the same conditions as Fig. 4(b). The maximal extinction ratio 39.07 dB is obtained at about $L_1 = 530$ nm. However, the peak in Fig. 4(c) is so flat, which proves that the influence of L_1 is less important for extinction ratio than L_2 . In other words, the present suppression is the primary vector to greater extinction ratio. Figure 4(d) shows the extinction ratio as a function of the incident wavelength at $L_1 = 530$ nm and $L_2 = 835$ nm. The maximal extinction ratio is 47.83 dB at $\lambda = 852$ nm, and the peak in Fig. 4(d) is quite higher and sharper, which may be applied in filter, etc. In the grating structure, the interaction of SPs between slits is much strong, hence more transmission power and extinction ratio are obtained than those in the single slit structure.

To check the single-pass effect caused by SPs in detail, the time-average distribution of near-field electric field intensity $|E|^2$ is simulated, as shown in Fig. 5. Figure 5(a) shows the distribution of $|E|^2$ depending on the enhancement of SPs to transmission T_1 . It is clearly observed that electric field of high intensity distributes on both surfaces of grating, which just proves that energy has effectively transmitted through slits. The opposite situation of transmission T_2 is shown in Fig. 5(b). The electric field only localizes on the lower surface of grating. No electric field can be observed in the slits or on the upper surface, which proves that scarcely any energy can transmit through slits in that direction. Hence the transmission T_2 is strongly inhibited and result in the single-pass effect.

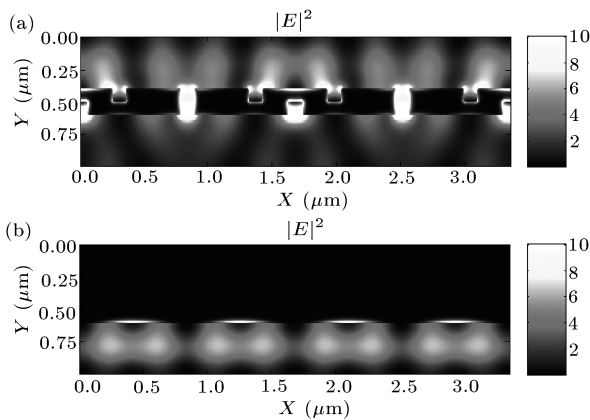


Fig. 5. The near-field electric field time-average distribution of $|E|^2$, i.e. transmissions (a) T_1 and (b) T_2 at the maximal extinction ratio of 47.83 dB. The incident light illuminates the grating from top to bottom in (a) and from bottom to top in (b). The lateral scale is two periods of grating. The parameters are chosen as $L_1 = 530$ nm, $L_2 = 835$ nm, $p = 2L_2 = 1670$ nm and incident wavelength $\lambda = 852$ nm.

In the grating structure, for simplicity of calculation, we only add two and one grooves on upper and under surfaces respectively between two slits. We believe that more extinction ratio can be obtained by optimizing structure parameters further. Although incident wavelength about $\lambda = 850$ nm is used in our work, this structure can be applied in any wavelength by changing related parameters, including the wavelength about $\lambda = 1550$ nm for communication.

In conclusion, we have investigated the optical single-pass effect in novel subwavelength metallic structures caused by SPs. Two main structures, single slit and grating structure with grooves on surfaces, have been discussed in detail. Influences of parameters of the structures on far-field transmission, near-field electric field distribution and extinction ratio are numerical studied by the FDTD method. Compared with the single slit structure, more transmission power and greater extinction ratio have been obtained with the grating structure, owing to the stronger interaction of SPs between slits and grooves. As a result, a maximal extinction ratio of 47.83 dB has been achieved in the grating structure. It is expected that our works are helpful for designing new optical instruments and contribute to more applications.

References

- [1] Ebbesen T W, Lezec H J, Ghaemi H F, Thio T and Wolff P A 1998 *Nature* **391** 667
- [2] Barnes W L, Dereux A and Ebbesen T W 2003 *Nature* **424** 824
- [3] Maier S A and Atwater H A 2005 *J. Appl. Phys.* **98** 011101
- [4] Lezec H J, Degiron A, Devaux E, Linke R A, Martin-Moreno L, Garcia-Vidal F J and Ebbesen T W 2002 *Science* **297** 820
- [5] García-Vidal F J, Lezec H J, Ebbesen T W and Martin-Moreno L 2003 *Phys. Rev. Lett.* **90** 213901
- [6] Lockyear M J, Hibbins A P, Sambles J R and Lawrence C R 2005 *J. Opt. A: Pure Appl. Opt.* **7** 152
- [7] Degiron A and Ebbesen T W 2004 *Opt. Exp.* **12** 3694
- [8] Jiao X J, Wang P, Tang L, Lu Y, Li Q, Zhang D G, Yao P J, Ming H and Xie J P 2005 *Appl. Phys. B* **80** 301
- [9] Lee K G and Park Q H 2005 *Phys. Rev. Lett.* **95** 103902
- [10] Schouten H F, Kuzmin N, Dubois G, Visser T D, Gbur G, Alkemade P F A, Blok H, Hooft G W, Lenstra D and Eliel E R 2005 *Phys. Rev. Lett.* **94** 053901
- [11] Lalanne P and Hugonin J P 2006 *Nature Phys.* **2** 551
- [12] Palik E D 1985 *Handbook of Optical Constants of Solids* (New York: Academic)
- [13] Taflove A and Hagness S 2000 *Computational Electrodynamics: The Finite-Difference Time-Domain Method* (Boston: Artech House)
- [14] Jubkins J B and Ziolkowski R W 1995 *J. Opt. Soc. Am. A* **12** 1974
- [15] Harms P, Mittra R and Ko W 1994 *IEEE Trans. Antennas Propagat.* **42** 1317
- [16] Berenger J P 1994 *J. Comput. Phys.* **114** 185